

Novel Photocatalytic Reactor for Water Purification

Ajay K. Ray and Antonie A. C. M. Beenackers

Dept. of Chemical Engineering, University of Groningen, 9747 AG Groningen, The Netherlands

A novel photocatalytic reactor design for water treatment is characterized by the use of new extremely narrow diameter lamps, thus allowing for much higher surface area for catalyst coating per unit reactor volume and consequently for much higher specific reactor capacity. Experiments in a reactor containing 21 novel U-shaped lamps coated with catalyst showed a 695% increase in efficiency of the reactor performance in comparison with a classical annular reactor and 259% in comparison with a slurry reactor. Both a classical annular reactor and a slurry reactor cannot be scaled up for large-scale applications due to the low values of illuminated catalyst surface area per unit volume of liquid treated inside the reactor while this configuration is flexible enough for large-scale applications.

Introduction

Water treatment processes based on aqueous phase hydroxyl radical chemistry (Ollis et al., 1991; Hagfeldt and Grätzel, 1995) are becoming powerful oxidation methods that can completely destroy (mineralize) almost all toxic organic compounds in water. Heterogeneous photocatalysis (Fox and Dulay, 1993; Mills et al., 1993) is one of the advanced oxidation processes that couples low energy ultraviolet light with semiconductors acting as photocatalysts, and has emerged as a viable alternative for solving environmental problems overcoming many of the drawbacks that exist for the traditional water treatment methods (Matthews, 1992). One of the major advantages of the photocatalytic process (Ollis et al., 1989) is the prospect of complete breakdown of organic pollutants to yield CO_2 , H_2O , and mineral acids. These include aliphatics, aromatics, polymers, dyes, surfactants, pesticides, and herbicides.

Photocatalytic reactions are promoted by solid photocatalyst particles, which are either dispersed in the liquid (Matthews, 1992) or immobilized on a surface (Zeltner et al., 1993). However, the use of suspensions requires the separation and recycling of the ultrafine catalyst from the treated liquid and can be an inconvenient, time-consuming expensive process. In addition, the depth of penetration of UV light is limited because of strong absorptions by both catalyst particles and

dissolved organic species. The above problems can be avoided in stationary photoreactors in which photocatalyst particles are immobilized onto a fixed surface such as the reactor wall, fiber mesh, glass or ceramic beads that are held in fixed positions in the photoreactor. However, immobilization of a semiconductor on a support generates a unique problem. The low interfacial surface area of the photocatalyst may lead to mass-transfer limitation problems. Glass beads or fiberglass mesh structures may increase the surface area available for catalyst but not the activated photocatalyst surface area, because of the opaque nature of the catalyst to UV light. Therefore, there is a need for a reactor whose design provides a high ratio of illuminated immobilized catalyst to illuminated surface and provides the possibility of total reactor illumination. The reactor described in this article provides a candidate solution to this problem.

In recent years, several review articles (Fox and Dulay, 1993; Mills et al., 1993; Legrini et al., 1993; Hoffmann et al., 1995) have appeared on photocatalytic water treatment with generally positive results indicating potential of photocatalytic oxidation technologies for very diverse categories of toxic compounds in water. However, technical development to pilot-scale level has not been successfully achieved although numerous patents have been approved worldwide. Based on the arrangement of the light source and reactor vessel, all these reactor configurations fall under the categories of *immersion* type with lamp(s) immersed within the reactor, *external* type with lamps outside the reactor or *dis-*

Correspondence concerning this article should be addressed to A. K. Ray at this present address: Dept. of Chemical Engineering, National University of Singapore, 10 Kent Ridge Crescent, Singapore 119260.

Table 1. Illuminated Catalyst Surface Area per Unit Volume of Liquid Treated Inside the Reactor, κ

Photocatalytic Reactor	$\kappa, \text{m}^2/\text{m}^3$	Parameters	κ, m^{-1}	Scale-Up
Slurry reactor	$\left[\frac{6C_c}{\rho_c} \right] \frac{1}{d_p}$	$d_p = 0.3 \mu\text{m}$ $C_c = 0.5 \text{ kg/m}^3$	2,631*	Not possible
External type annular reactor	$\frac{4d_o}{d_o^2 - d_i^2}$	$d_o = 0.2 \text{ m}$ $d_i = 0.1 \text{ m}$	27	Not possible
Immersion type with classical lamps	$\left[\frac{4\epsilon}{1 - \epsilon} \right] \frac{1}{d_o}$	$d_o = 0.09 \text{ m}$ $\epsilon = 0.75$	133	Possible, but large V_R
Immersion type with new lamps	$\left[\frac{4\epsilon}{1 - \epsilon} \right] \frac{1}{d_o}$	$d_o = 0.0045$ $\epsilon = 0.75$	2,667	Possible, with small V_R

*The value will be much lower than $2,631 \text{ m}^{-1}$ as all the suspended catalyst particles will not be effectively illuminated. Catalyst concentration C_c of 0.5 kg/m^3 is normally used. ρ_c is equal to $3,800 \text{ kg/m}^3$.

tributive type with the light distributed from the source to the reactor by optical means such as reflectors or optical fibers. The majority of reactors patented are in fact a variation of the classical annular reactor of the immersion or the external type in which the catalyst is immobilized on the reactor wall (Sato, 1992; Taoda, 1993), on pipes internally (Matthews, 1990), on ceramic membranes (Anderson et al., 1991), on the glass wool matrix between plates (Cooper, 1989), on semipermeable membranes (Miano and Borgarello, 1991; Oonada, 1994), embedded in water permeable capsules (Hosokawa and Yukimitsu, 1988), on a mesh of fiberglass (Henderson and Robertson, 1989), on beads (Heller and Brock, 1993), on fused silica glass fibers (Hofstadler et al., 1994), on porous filter pipes (Haneda, 1992), on glass fiber cloth (Masuda et al., 1994), and so on. The reactors are either helical (Ritchie, 1991), spiral (Matthews, 1988), shallow cross-flow basins (Cooper and Ratcliff, 1991) or optical fiber (Wake and Matsunaga, 1994; Peill and Hoffmann, 1995). However, none of these has been successfully brought out of the laboratory yet. All these reactor designs are limited solely to small scales by the low values of total illuminated catalyst surface area per unit volume of liquid treated inside the reactor (Table 1) and the only way to apply these systems for large-scale applications is by using large numbers of multiple units. In this article a novel reactor design is presented that allows for a much higher illuminated surface area per unit reactor volume and is flexible enough to be scaled up for commercial scale applications.

Major Challenges in the Development of Photocatalytic Reactor

The problem of scale-up of multiphase photocatalytic reactors is more complex than that of conventional chemical reactors or homogeneous photoreactors. In fact, in photocatalytic reactor development, besides conventional reactor scale-up complications such as mixing, mass transfer, reaction kinetics, catalyst installation, and so on, an additional engineering factor related to illumination of catalyst becomes relevant. This is the process of photon energy absorption. The high degree of interaction between the transport processes, reaction kinetics, and light absorption leads to a strong coupling

of physicochemical phenomena, and there is no doubt that it is a major obstacle in the development of efficient photocatalytic reactors.

The central problem in a photocatalytic reactor is focused on a uniform distribution of light to a large surface area of catalyst. For a particular photoreactor geometry, scale-up in the axial and/or radial directions is constrained by the phenomenon of opacity, light scattering, depth of radiation penetration and local volumetric light absorption. The arrangement of the light source-reactor system influences the reactor design in such a strong way that independent consideration is not possible. Moreover, the need for at least one of the reactor walls to transmit the chosen radiation imposes the utilization of transparent materials, such as glass for the reactor construction, and thus imposes size limitations, sealing problems, and breakage risks.

The overall rate of reaction of photocatalytic processes which usually follow Langmuir-Hanshelwood kinetics is slow compared to conventional chemical reaction rates due to the low concentration levels of the pollutants and, therefore, there is a need to provide large amounts of active catalyst inside the reactor. Even though the internal surface area of the porous catalyst is high, there can only be a thin coating (about $1 \mu\text{m}$ thick) applied to a carrier surface. Thus, the amount of active catalyst in the reactor is limited and, even if individual degradation processes can be made relatively efficient, the overall conversion efficiency will still be low. This problem severely restricts the processing capacity of the reactor and the necessary time required to achieve high conversions are measured in hours, if not days.

For comparison of design efficiency of different photocatalytic reactors in terms of their efficacy to install as much as activated catalyst per unit volume of reaction liquid inside the reactor, the author proposes a parameter κ , namely illuminated specific surface area, representing the total illuminated surface area of catalyst within the reactor that is in contact with the reaction liquid. Table 1 (see Appendix 1) lists κ values for three different classes of common photocatalytic reactors. These are a slurry reactor (SR), an external type reactor such as a classical annular reactor (CAR) in which a lamp is placed inside the inner tube while the reaction liquid is flowing through the annulus with the inside of outer annulus coated with catalyst, and an immersion type reactor in which several lamps coated with catalyst on their surface are immersed inside the reaction liquid. An external type reactor will always be limited with low values of κ . Whereas, in a slurry reactor, small catalyst particles could provide a large surface area for reaction but essentially most of the catalyst surface area will be inactive, as it will not receive enough light from external light source, particularly for large reactor dimensions. An immersion type reactor could be scaled up to any dimension, but when classical lamps of diameter between 0.07 to 0.1 m are used the κ value is not very high even if it is assumed that 75% of the reactor volume is occupied with the lamps. In order to overcome the deficiencies inherent in conventional photochemical reactor designs, we present a novel configuration that allows not only a much higher value for κ but also the catalyst can be activated uniformly at its highest possible level. Moreover, the reactor design is flexible enough to be scaled up for large-scale applications.

Basic Concept of the Reactor

The concept is based on a unique new lamp design developed by Philips. These are extremely narrow diameter fluorescent tube lamps of low wattage emitting lights in the wavelength of our interest ($\lambda < 380$ nm). These lamps are available in various shapes and lengths, and can be placed inside a reactor to form a variety of different configurations. The photocatalytic reactor is described here as the tube light reactor (TLR). Since the lamps are extremely narrow in diameter, evidently a very large number of such lamps can be placed inside the reactor. In the present reactor configuration, the catalyst was deposited on the outer surface of these low wattage lamps and thus provides a high light transfer area and allows for a higher illuminated specific catalyst surface area than even a slurry reactor. Another potential advantage of distributing light is that light does not have to pass through the reactant and product phases in the reactor. This is advantageous because when light approaches the catalyst through the bulk liquid phase, some radiation is lost due to absorption in the liquid. This effect is more pronounced for highly colored dye pollutants as they are a strong UV absorber and will, therefore, significantly screen the TiO_2 from receiving UV light. Of course, this is possible with classical lamps too. However, the new lamps allow for a 10 to 20 times larger surface area for catalyst per unit reactor volume compared to a classical reactor design (Table 1).

Experimental Details

Reactor

The reactor (Figure 1) consists of a stainless steel flat top plate ($0.132 \text{ m} \times 0.016 \text{ m}$) with 21 holes onto which another plate ($0.248 \text{ m} \times 0.132 \text{ m}$) was welded. 21 U-shaped lamps

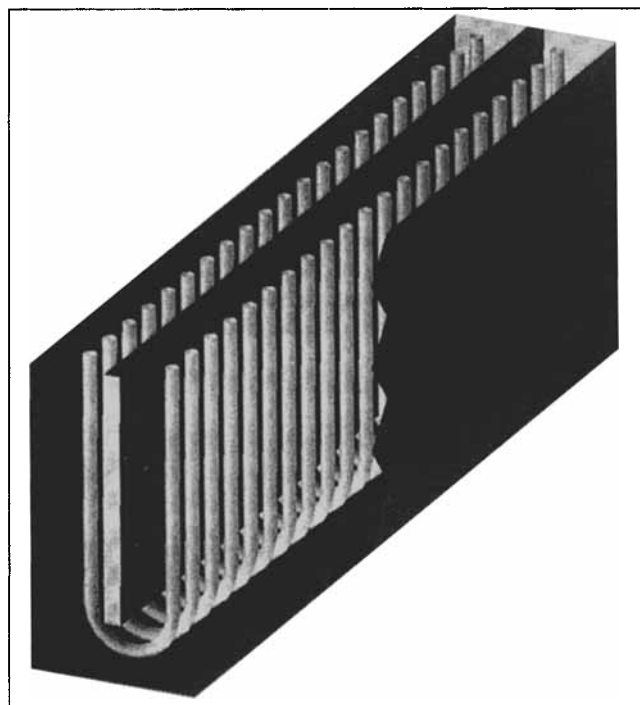


Figure 1. Tube light reactor (TLR).

were placed around the latter plate and its end extended through the holes for electrical connections. Electrical wires were connected to the novel lamps through copper holders that are screwed around the lamps end. This part acts as a clamp for the lamps. The assembly was put in a rectangular stainless steel reactor vessel. Feed is introduced at the top of the vessel and is equally distributed over the width of the reactor through five inlet ports thereby minimizing formation of any dead zones. Similarly, the flow exits the reactor through five ports at the other end. The effective illuminated surface areas of the catalyst and the volume of the reactor are 0.15 m^2 and $5.36 \times 10^{-4} \text{ m}^3$, respectively. The parameter κ , defined as total illuminated catalyst surface area that is in contact with reaction liquid per unit volume of liquid treated in the reactor volume, is equal to $618 \text{ m}^2/\text{m}^3$.

Lamps

The novel lamps (Philips NDF-U2 49-6W) used were specially developed by Philips Lighting for our experiments. The U-shaped lamps are 0.498 m long and have a diameter of 0.0045 m only. These operate at $1,020 \text{ V}$, and produce 6 W of which 15% is in the UV-A region. The light intensity ($\lambda < 380 \text{ nm}$) on catalyst particles is $127.8 \text{ W}/\text{m}^2$.

Experimental setup

A gear pump (Verder model 2036; maximum flow rate of $3.0 \times 10^{-5} \text{ m}^3/\text{s}$) circulated the reactant between the reactor and the reservoir via a flow-through cuvette placed inside a photometer (Vitatron 6000) for continuous on-line measurement of the model component (Figure 2). Two three-way glass valves were used between the water and specially designed reactant reservoir for initial zero setting of the analytical instrument before the start of an experiment, introduction of

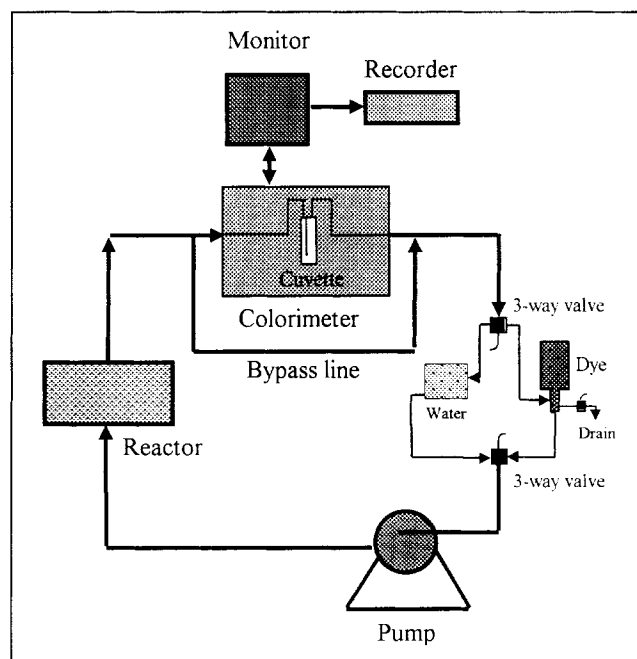


Figure 2. Experimental setup.

the reactant into the system, elimination of bubbles formed during experiment, and final flushing of the entire system. The reactor assembly was placed inside a thermostat bath.

Catalyst

Degussa P25 grade TiO_2 was used as a catalyst for all the experiments. The crystalline product is nonporous primarily in the anatase form (70:30 anatase to rutile) and is used without further treatment. It has a BET surface area of $(5.5 \pm 1.5) \times 10^4 \text{ m}^2/\text{kg}$ and crystallite sizes of 30 nm in 0.1–0.3- μm -dia. aggregates.

Catalyst immobilization

For better catalyst fixation and its durability, the glass surface of the lamps was roughened by sand blasting. This makes the catalyst surface uneven but increases the strength and amount of catalyst per unit area that could be deposited. The lamp surface was carefully degreased, cleaned with 5% HNO_3 solution overnight, and washed with water and then dried. A 5% aqueous suspension of the catalyst was prepared with water out of Millipore Milli-Q water purification system. The suspension was mixed in an ultrasonic cleaner (Branson 2200) bath to obtain a milky suspension that remained stable for weeks. The lamp's surfaces were coated with catalyst by dip-coating apparatus (Figure 3) designed for coating catalyst.

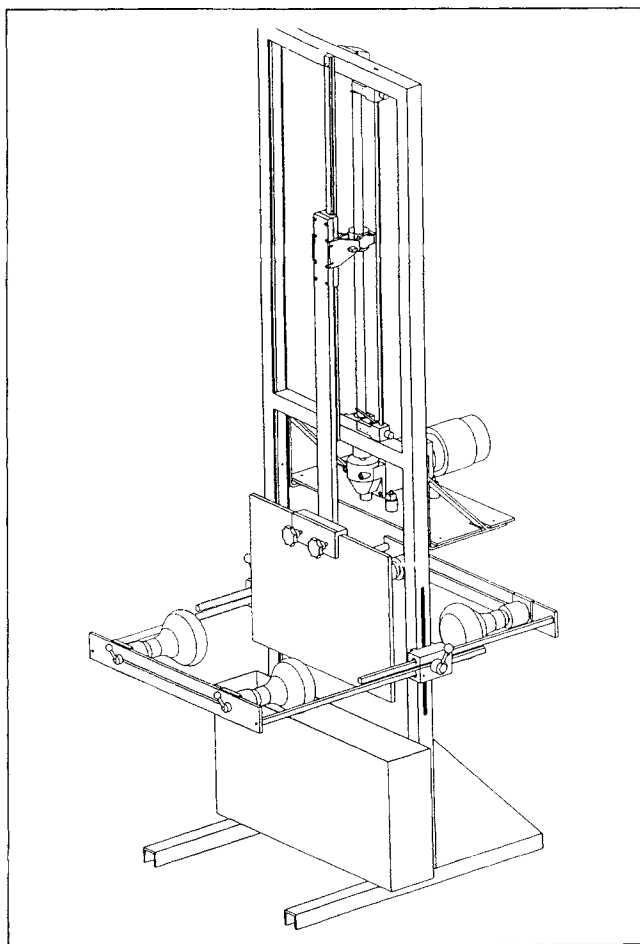


Figure 3. Dip-coating apparatus.

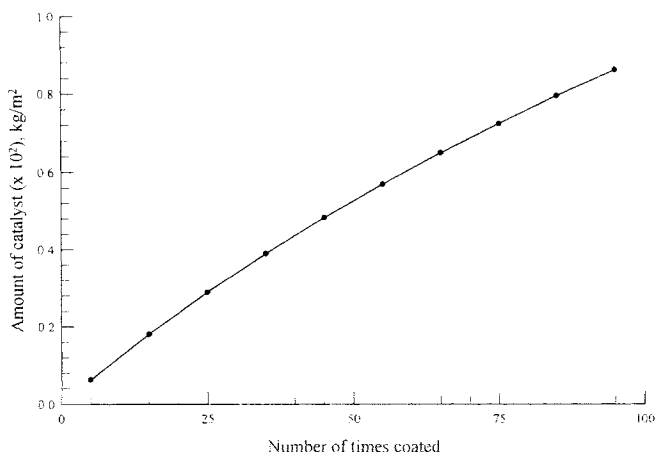
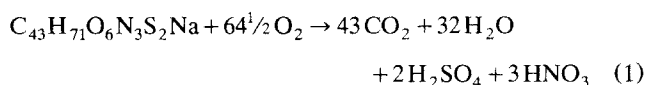


Figure 4. Catalyst layer thickness with number of coatings.

This is a completely automated equipment capable of immobilizing the catalyst onto a variety of different shaped and sized substrates to any desired thickness by successive dipping of the objects into a suspension at controlled speed that can be varied between $(0.4\text{--}4.0) \times 10^{-4} \text{ m/s}$. Four 250 W infrared lamps were attached to a clamp that can be moved both vertically and horizontally for instant drying of the coating. Figure 4 shows the amount of catalyst immobilized per unit area with the number dipping.

Model component

Special Brilliant Blue of Bayer (SBB, MW 812) of laboratory reagent grade (in 20% solution) was used (catalog number 42735). This is an excellent model component for characterization of a photocatalytic reactor as the dye is reactive only in the presence of both TiO_2 and UV light, biologically not degradable, and present in wastewater streams from textile industries. The complete oxidation reaction of SBB dye is



Analysis

Changes in SBB dye concentration were measured on-line by flowing a bypass stream of the dye from the reactor outlet continuously through a bottom loader flow-through cuvet (Hellma, path length 0.001 m) placed inside a Colorimeter (Vitatron Universal Photometer 6000) and was recorded continuously by a Kipp and Zonen (Model BD80) recorder. Up to 0.5 mol/m^3 , the calibration line obeys the Beer-Lambert law with good precision and the absorptivity coefficient ϵ (at $\lambda_{\text{max}} = 605 \text{ nm}$) was found to be $5,000 \text{ m}^3/\text{mol/m}$.

Experimental procedure

At the start of every experiment, the reactor was rinsed with Milli-Q water before zero-setting the analytical instrument. The reactor was then filled with the dye solution, and it was ensured that no air bubbles remained in the system.

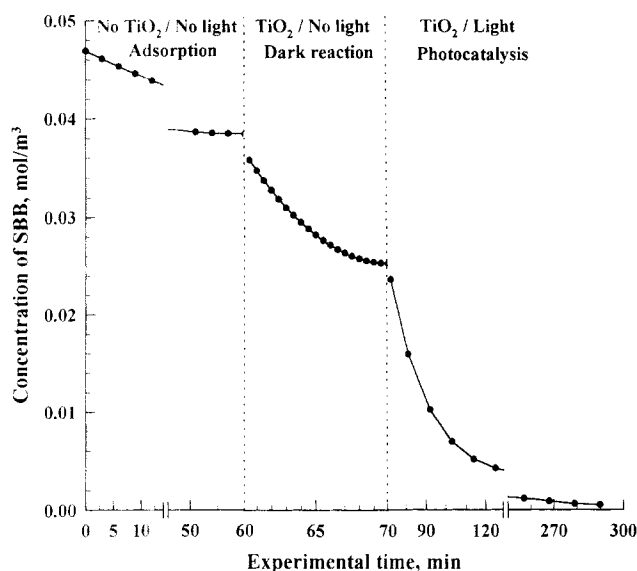


Figure 5. Typical experiment showing adsorption of the dye in the system, dark reaction and photocatalysis.

The change in the dye concentration was continuously recorded. New silicon connecting tubes and fresh catalyst were found to absorb the dye for about an hour, but no noticeable adsorption by the entire system was observed afterwards. Light was turned on only when the colorimeter reading was stabilized. A typical experimental result is shown in Figure 5. The decrease in concentration in the first two parts can be attributed to the adsorption of the dye by the connecting tubing (no catalyst present) and fresh catalyst, respectively, while that of the last part was when light was turned on and actual photocatalysis occurred.

Evidence of complete mineralization

The COD for SBB dye is given by

$$\text{COD} = y \cdot [M_{\text{Oxygen}}/M_{\text{SBB dye}}] \cdot n = 2.542 y \quad (2)$$

where y is the concentration of the SBB dye in ppm, M_{Oxygen} and $M_{\text{SBB dye}}$ are the respective molecular weights and n for the dye is $64^{1/2}$. COD was measured for various virgin dye solutions for liquid collected at the end of several experiments and for pure Milli-Q water. COD values for the virgin solutions were always equal to the value calculated from Eq. 2 and that of the treated liquid and blank was zero. COD value for the final treated liquid shows that complete mineralization occurred and for the present model component colorimetric analysis was justified as it was not merely measuring the decolorization of the dye.

Experimental results

Experiments with increased flow rate caused an increase in the conversion rate (Figure 6) showing influence of external mass transfer. For most experiments, a flow rate of $1.67 \times 10^{-5} \text{ m}^3/\text{s}$ was used as higher flow rates introduced bubbles inside the reactor.

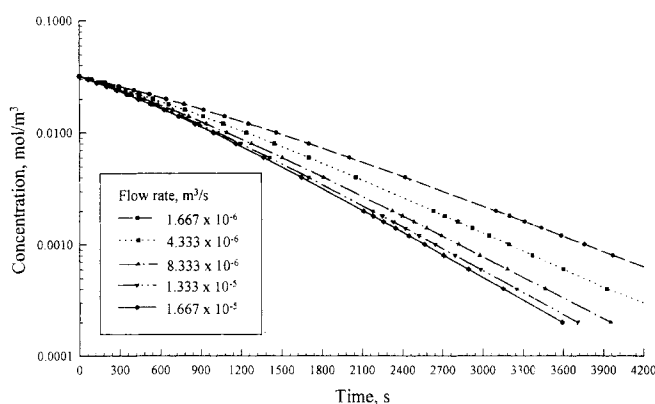


Figure 6. Influence of external mass transfer (flow rate) on the overall rate.

Figure 7 shows experimental results for the photocatalytic destruction of SBB for various starting concentrations. The figure reveals that 90% of the pollutant was degraded in about 30 min. The efficiency of the reactor, expressed in terms of mols converted per unit time per unit reactor volume per unit electrical power consumed, is compared with two different reactors (Assink et al., 1993), namely a slurry reactor and a classical annular reactor, for the same initial concentration ($C_o = 0.024 \text{ mol/m}^3$) of the SBB dye. The slurry reactor consists of 20 tubes each of volume $7 \times 10^{-5} \text{ m}^3$ containing $3 \times 10^{-5} \text{ m}^3$ of liquid (with TiO_2 concentration of 0.5 kg/m^3) placed on a holder that rotates around a magnetic stirrer and was surrounded by 24 Philips TLK 40W/10R lamps. The annular reactor was of 0.099 m outside and 0.065 m inside diameter with 0.77 m long surrounded externally with 10 Philips TLK 40W/10R lamps. When the efficiency of the test reactor is compared (Table 2) with the classical annular reactor, an increase of about 695% was observed while an increase of 259% was observed when compared to the slurry reactor in spite of the fact that the slurry reactor offers a much higher κ value. This increase in efficiency is in spite of the fact that the design of this test reactor was far from optimum with

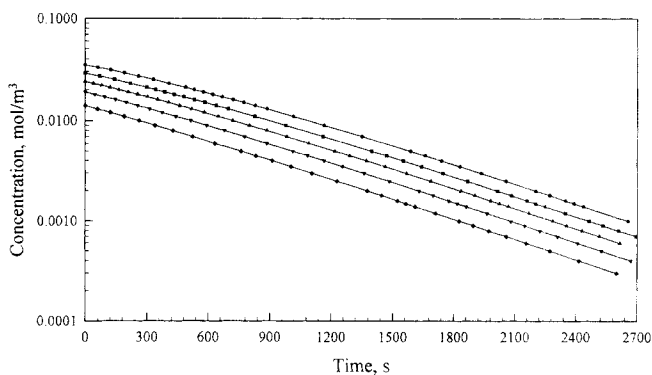


Figure 7. Photocatalytic degradation of SBB dye for various initial concentration.

Reactor specification: volume of reactor = $5.36 \times 10^{-4} \text{ m}^3$; illuminated catalyst surface area = 0.15 m^2 ; number of lamps = 21; catalyst amount = $4.0 \times 10^{-3} \text{ kg/m}^2$; experimental condition: flow rate = $1.67 \times 10^{-5} \text{ m}^3/\text{s}$; volume of liquid treated = $4.05 \times 10^{-4} \text{ m}^3$.

Table 2. Reactor Specifications, Experimental Conditions, and Reactor Performance Efficiency for CAR, SR, and TLR

	Classical Annular Reactor (CAR) [†]	Slurry Reactor (SR) [‡]	Tube Light Reactor (TLR) [‡]
Vol. of reactor, m ³	3.48×10^{-3}	1.4×10^{-3}	5.36×10^{-4}
Cat. surface area, m ²	0.18	3.7	0.15
Parameter κ , m ² /m ³	69	6,139**	618
Vol. flow rate, m ³ /s	8.42×10^{-5}	Batch operation	1.67×10^{-5}
Electr. energy input, W	400	960	126
Eff.*, $\mu\text{mol/s/m}^3/\text{W}$	9.50×10^{-3}	2.10×10^{-2}	7.55×10^{-2}
% increase in eff.	1	121	695
Scale-up	no	no	yes

*Efficiency is expressed as 90% pollutant (SBB dye) converted ($\mu\text{mol/s}$) from a starting concentration of 0.024 mol/m^3 per unit reactor volume (m^3) per unit electrical energy (W) used.

**The value will be much lower than $6,139 \text{ m}^{-1}$ as all the suspended catalyst particles are not effectively illuminated and the assumption of average aggregate particle diameter of $0.3 \mu\text{m}$ may be too small.

[†]Assink et al. (1993).

[‡]This article.

respect to mass transfer, flow distribution, and efficiency of packing of the tube lamps inside the reactor. In addition, the novel reactor design has the capability of being scaled up to any dimensions whereas the other two reactors are restricted only to a small reactor capacity.

The catalyst coating on the lamp's surface appeared to be durable and the catalyst activity did not deteriorate even after 50 h of experimentation. A problem is still the burning stability and lifetime of the lamps, but it is expected that this will be improved in the months ahead. A comprehensive experimental program on the influence of operating parameters on the conversion rates is presently being carried out.

Conclusions

A new photocatalytic reactor design concept with a 100 to 150 fold increase in surface area per unit volume of reaction liquid inside the reactor relative to a classical annular reactor design and a 10 to 20 fold increase relative to immersion type reactor with classical lamps has been proposed and developed. In this article, experimental results based on a reactor configuration where new extremely narrow diameter artificial fluorescent lamps with a near UV spectra are used is presented. A simple laboratory-scale test reactor using these lamps was designed, constructed, and tested for overall performance evaluation. Experiments performed in a reactor of volume $5.36 \times 10^{-4} \text{ m}^3$ containing 21 novel U-shaped lamps of diameter 0.0045 m coated with catalyst showed a 695% increase in efficiency of the reactor performance when compared with a classical annular type photocatalytic reactor and 259% when compared with a slurry reactor. Both the classical annular reactor and the slurry reactor cannot be scaled up for large-scale applications due to the low values of illuminated catalyst surface area per unit volume of liquid treated inside the reactor while the present configuration is flexible enough for industrial scale applications.

Acknowledgment

We thank Thomas Van der Laan for experimental work and Luuk Balt for technical assistance. We also thank Philips Lighting for pro-

viding us with the new lamps. We acknowledge the financial support from the Netherlands Ministry of Economic Affairs, The Hague.

Notation

κ = illuminated catalyst density, m^2/m^3
 λ = wavelength, nm
 ρ = density, kg/m^3

Subscripts and superscripts

0 = outer
c = catalyst
max = maximum

Literature Cited

- Anderson, M. A., S. Tunesi, and Q. Xu, "Degradation of Organic Chemicals with Titanium Ceramic Membranes," U.S. Patent 5035784 A, 910730 (1991).
- Assink, J. W., T. P. M. Koster, and J. M. Slaager, "Fotokatalytische oxydatie voor afvalwaterbehandeling," Internal Report Reference No. 93-137, TNO-Milieu en Energie, Apeldoorn, The Netherlands (1993).
- Cooper, G. A., "Photocatalyst in a Glass Wool Matrix between Plates," U.S. Patent 4,888,101 (1989).
- Cooper, G. A., and M. A. Ratcliff, "System for and Method for Decontaminating a Contaminated Fluid by Using Photocatalytic Particles," WO 9108813 A1 910627 (1991).
- Fox, M. A., and M. T. Dulay, "Heterogeneous Photocatalysis," *Chem. Rev.*, **93**, 341 (1993).
- Hagfeldt, A., and M. Grätzel, "Light-Induced Redox Reactions in Nano-Crystalline Systems," *Chem. Rev.*, **95**, 49 (1995).
- Haneda, K., "Photocatalytic Element Pipe and Photocatalytic Chemical Reactor," Japanese patent JP 04061933 A2 920227 (1992).
- Heller, A., and J. R. Brock, "Materials and Methods for Enhanced Photocatalysis of Organic Compounds in Oil Spill Treatment," patent WO 9317971 A1 930916 (1993).
- Henderson, R. B., and M. K. Robertson, "Fluid Purification by Photodegradation of Organic Pollutants and Microorganisms," patent EP3063301 A1 890308 (1989).
- Hoffmann, M. R., S. C. Martin, W. Choi, and D. W. Bahnemann, "Environmental Applications of Semiconductor Photocatalysis," *Chem. Rev.*, **95**, 69 (1995).
- Hofstadler, K., R. Bauer, S. Novallé, and G. Helsler, "New Reactor Design for Photocatalytic Treatment with TiO_2 Immobilized on Fused-Silica Glass Fibers: Photomineralization of 4-Chlorophenol," *Environ. Sci. and Technol.*, **28**, 670 (1994).
- Hosokawa, M., and K. Yukimitsu, "Treatment of Waste Fluids with Titania Particles," patent JP 63042793 A2 880223 (1988).
- Legrini, O., E. Oliveros, and A. M. Braun, "Photochemical Processes for Water Treatment," *Chem. Rev.*, **93**, 671 (1993).
- Masuda, R., K. Kawashima, W. Takahashi, M. Murabayashi, and K. Ito, "Photocatalysts for Treatment of Harmful Substances and Its Apparatus," patent JP 06320010 A2 941122 (1994).
- Matthews, R. W., "Semiconductor Photocatalytic Method and System for Determining Organic Matter in an Aqueous Solution Including an Oxidizing Agent," U.S. Patent WO 8806730, Australian Patent A1 880907 (1988).
- Matthews, R. W., "Coating Photoactive Metal Oxides onto Substrates and Their Use in Water Purification," patent AU 600289 B2 900809 (1990).
- Matthews, R. W., "Photocatalytic Oxidation of Organic Contaminants in Water: An Aid to Environmental Preservation," *Pure and Appl. Chemistry*, **64**(9), 1285 (1992).
- Miano, F., and E. Borgarello, "Method for the Heterogeneous Catalytic Photodegradation of Pollutants," patent EP 417847 A1 910320 (1991).
- Mills, A., R. H. Davies, and D. Worsley, "Water Purification by Semiconductor Photocatalysis," *Chem. Soc. Rev.*, 417 (Dec. 1993).
- Ollis, D. F., E. Pelizzetti, and N. Serpone, *Photocatalysis: Fundamentals and Applications*, Wiley, New York (1989).
- Ollis, D. F., E. Pelizzetti, and N. Serpone, "Destruction of Water Contaminants," *Environ. Sci. Technol.*, **25**(9), 1523 (1991).

- Oonada, J., "Water Purifying Method," patent JP 06071256 A2 940315 (1994).
- Peill, N. J., and M. R. Hoffmann, "Development and Optimization of a TiO₂ Coated Fiber Optic Cable Reactor," *Environ. Sci. Technol.*, **29**, 2974 (1995).
- Ritchie, D. G., "Photocatalytic Fluid Purification Apparatus having Helical Nontransparent Substrate," patent US 5069885 A 911203 (1991).
- Sato, K., "Drinking Water Container Capable of Decomposing Organic Halogen Compounds by Light Irradiation," patent JP 04114791 A2 920415 (1992).
- Taoda, H., "Water Treatment," patent JP 05076877 A2 930330 (1993).
- Wake, H., and T. Matsunaga, "Redox Reaction Using Photocatalysis of Semiconductor," patent JP 06134476 A2 940517 (1994).
- Zeltner, W. A., C. G. Hill, and M. A. Anderson, "Supported Titania for Photodeg-Radiation," *ChemTech* (May 21, 1993).

External type reactor

A classical annular reactor is considered in which a lamp is placed inside the inner tube while the reaction liquid is flowing through the annulus and inside of the outer annulus is coated with catalyst. The κ can be calculated as

$$\kappa = \frac{\pi d_o L}{\frac{\pi}{4}(d_o^2 - d_i^2)L} = \frac{4d_o}{(d_o^2 - d_i^2)} \quad (3)$$

where d_o (m) and d_i (m) are the outside and inside diameter of the annulus, respectively, and L (m) is the length of the reactor.

Immersion type reactor

An immersion type reactor is considered in which several lamps of diameter d_o (m) coated with catalyst on its surface are immersed inside the reaction liquid. If ϵ is defined as the fractional volume of the reactor occupied by the lamps, then $V_{\text{lamps}} = \epsilon V_R$ and $V_L = (1 - \epsilon)V_R$. Also, the surface area to volume ratio is equal to $A_{\text{lamps}}/V_{\text{lamps}} = 4/d_o$. The κ can be calculated as

$$\kappa = \frac{A_{\text{lamps}}}{V_L} = \frac{A_{\text{lamps}}}{(1 - \epsilon)V_R} = \frac{\epsilon A_{\text{lamps}}}{(1 - \epsilon)V_{\text{lamps}}} = \left[\frac{4\epsilon}{(1 - \epsilon)} \right] \frac{1}{d_o} \quad (4)$$

Manuscript received Feb. 24, 1997, and revision received June 2, 1997.

Appendix 1: Calculation of κ for Different Reactors

Slurry reactor

A mass balance for the catalyst particles results

$$\left[\frac{\pi d_p^3}{6} \right] N_p \rho_c = C_c V_L \quad (1)$$

where d_p and N_p are the particle diameter (m) and number of particles respectively, ρ_c (kg/m³) and C_c (kg/m³) are the density and concentration (mol/m³) of catalyst, respectively, and V_L (m³) is the volume of liquid inside the reactor. The κ can be calculated as

$$\kappa = \frac{\pi d_p^2 N_p}{V_L} = \pi d_p^2 \left[\frac{6C_c}{\pi d_p^3 \rho_c} \right] = \left[\frac{6C_c}{\rho_c} \right] \frac{1}{d_p} \quad (2)$$